Journal of
Instrumentation

Graphene growth from commercial Kapton by direct laser scribing studied by confocal micro-Raman spectroscopy, laser confocal and atomic force microscopies

To cite this article: Sabina Botti *et al* 2025 *JINST* **20** C09008

Published by IOP Publishing for Sissa Medialab

Received: *February 18, 2025*
Revised: *June 21, 2025*
Accepted: *July 21, 2025*
Published: *September 16, 2025*

7th International Conference Frontiers in Diagnostic Technologies
INFN research center of Frascati, Italy
21–23 October 2024

2025 JINST 20 C09008

Graphene growth from commercial Kapton by direct laser scribing studied by confocal micro-Raman spectroscopy, laser confocal and atomic force microscopies

Sabina Botti[a,*] **Francesca Bonfigli**[a] **Alessandro Rufoloni**[a] **Angelo Vannozzi**[a] **and Alessio Bruttomesso**[b]

[a] *ENEA, Nuclear Department,*
Via E. Fermi 45, 00044, Frascati, Italy
[b] *Optoprim s.r.l.,*
via dei Quadri 42/44, 20871 Vimercate (MB), Italy

E-mail: Sabina.Botti@enea.it

Abstract: In this work, direct laser scribing tests irradiating a commercial Kapton tape with nanosecond UV laser have been performed to investigate a Laser-Induced Graphene (LIG) process. Laser writing powers were changed to investigate the light-material interactions in LIG fabrication processes and to optimize the experimental parameters. LIG lines were characterised by confocal micro-Raman spectroscopy, laser confocal and atomic force microscopies gaining a deep insight on transient formation process of LIG and helping the identification of critical parameters that govern this process. The present study investigates the effects of the laser processing parameters on the LIG quality, with consequent process optimization confirming that LIG is a low-cost straightforward method to directly fabricate graphene sheets on a carbon-rich substrate that will have a growing importance in a near future.

Keywords: Imaging spectroscopy; Lasers

*Corresponding author.

https://doi.org/10.1088/1748-0221/20/09/C09008

Contents

1 Introduction

LIG is prepared by single step laser writing processes on many carbonaceous materials [1, 2]. Laser scribing on a polymeric material, such as polyimmide (Kapton), induces a breaking of C-O, C=O and C-N bonds, with consequent rearrengement of carbon atoms to form a graphene structure, depending on the laser wavelength (IR or UV) the pristine bonds are broken by pyrolisis or by photolysis process [3]. The adoption of ultraviolet laser-induced graphene (UV-LIG) writing presents notable advantages for the development of high-performance wearable sensors. Unlike traditional laser-induced graphene methods that employ infrared or CO_2 lasers, UV-LIG leverages the high photon energy of ultraviolet light to induce localized photothermal and photochemical conversion of carbon-rich precursors at lower temperatures. This is particularly beneficial for wearable electronics, which often require fabrication on flexible, thermally sensitive substrates such as polyimide (PI), polyethylene terephthalate (PET), or even biodegradable materials like cellulose paper [4].

A key advantage of UV-LIG for wearable sensors lies in its higher patterning resolution, stemming from the shorter wavelength of UV light. This allows for the fabrication of fine, microscale graphene features, enabling miniaturized and densely packed sensing arrays [5–8]. To gain a deep insight on transient formation process of LIG and identification of critical parameters that govern this process it is important to define a characterisation protocol that is affordable, fast and easy to handle. The UV-LIG structures reported in this work were characterised by confocal micro-Raman spectroscopy with surface scanning, confocal laser scanning (CLSM) and atomic force (AFM) microscopies. The Raman spectroscopy can follow the onset of Kapton carbonisation by increasing laser power and gives information on the quality of formed graphene, whereas the CLSM and AFM measured the penetration depth of laser into Kapton.

2 Materials and methods

Graphene straight lines were produced by UV laser writing process with a scanning speed of 5 mm/s, by focusing the UV laser (INNOLAS, maximum power = 5 W, pulse width 5–8 ns, repetition rate 20–200 kHz, F-theta lens = 100 mm, theoretical laser spot 10 µm) on the Kapton surface at different irradiating laser powers. Raman maps were acquired with a confocal micro-Raman spectrometer (Horiba XploRA Plus) with a 532 nm-wavelength laser. The Raman signals were collected through microscope equipped with 5×, 10×, 50×, and 100× objectives. Laser power can be attenuated by neutral density filters. The Raman spectra reported in this paper were obtained under the following conditions: laser power 15 mW, accumulation time 1 s, range 100–3500 cm^{-1}, The recorded spectra

were background subtracted and smoothed. Optical images were acquired with a confocal laser scanning microscope (CLSM) Nikon 80i-C1 operating in reflection mode, illuminating with a 532-nm laser (with nominal output power of 3 mW) and the reflected signal was directly detected by a photomultiplier. A set of 2D images at different Z positions were detected for a Z interval = 0–30 µm, Z step = 1 µm, XY = (315 × 315) μm^2 (objective 40×). The software of the confocal microscope, after acquisition of the 2D slices, performs a 3D reconstruction of the images [3]. Surface analyses were performed with Park System XE-150 Atomic Force Microscope (AFM) operating in non-contact mode. Pre-mounted non-contact, high-resolution cantilevers working at 309 MHz with nominal tip radius below 10 nm were used. Images were flattened by subtracting a linear background for the fast scan direction and a quadratic background for the slow scan direction.

3 Results and discussions

Figure 1 reports the optical image of three straight lines produced with UV laser writing process at increasing powers (named lines 1, 2, 3) detected by the CLSM in reflection mode. Their 3D reconstructions obtained by CLSM are reported in figure 2.a, b, c, where the false colours scale from blue to red are referred to Z scan values from 0 to 30 µm. The corresponding intensity profiles of the images detected on the surface along the width of the lines are reported in figure 3. By increasing the writing laser power, the LIG line width increases: ~16 µm for line 1, ~40 µm for line 2, ~70 µm for line 3, while the depths remain almost constant.

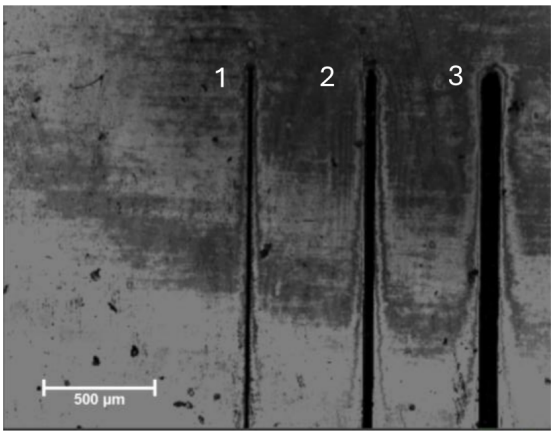

Figure 1. Optical images of the three UV lines detected by the CLSM in reflection mode.

Figure 4 reports the AFM analysis. The shapes of the line borders change with the writing laser power and line 3 exceeds the scanning range of AFM, however the measured line widths are in fair agreement with those obtained by CLSM measurements as shown in figure 3.

The Raman spectra obtained on the three LIG lines are reported in figure 5.a with Kapton Raman trace before laser irradiation. At lower laser power as in the case of lines 1 and 2, besides D, G and 2D bands that are characteristic features of graphene, still appear bands of Kapton. These Kapton bands are not present in the Raman spectra taken from line 3. Looking at optical microscope images of three lines reported in figure 1 we can observe that a black material is formed by UV laser scribing, but by using Raman spectroscopy we can discriminate between the formation of a mixed phase and the formation of graphene when the 2D band appears.

2025 JINST 20 C09008

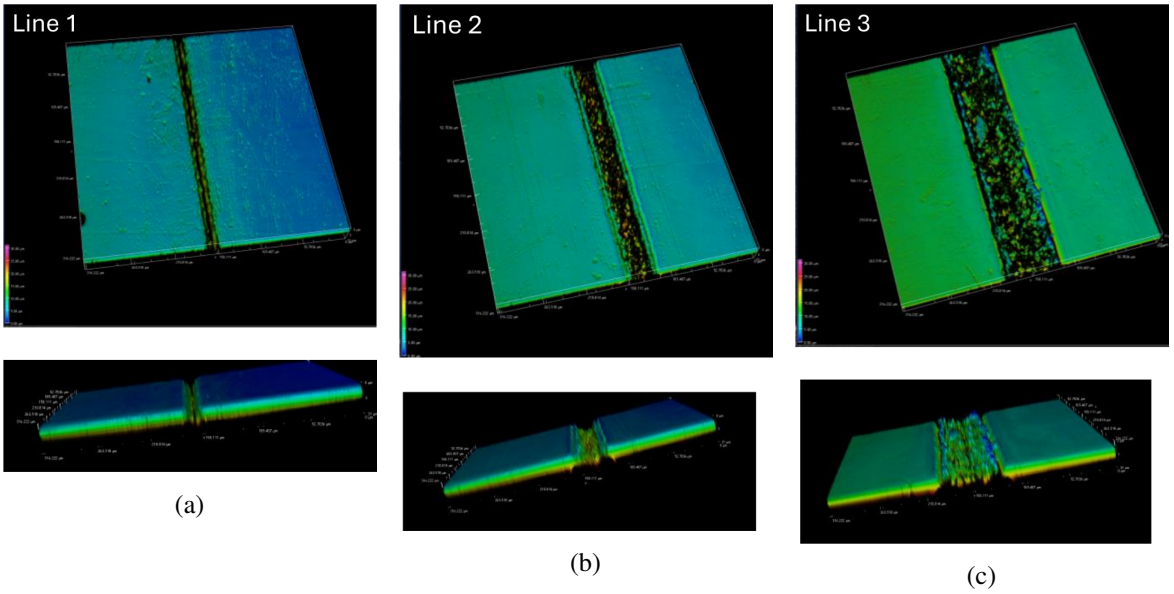

Figure 2. (a), (b), (c) 3D reconstructions obtained by CLSM of lines 1, 2, 3.

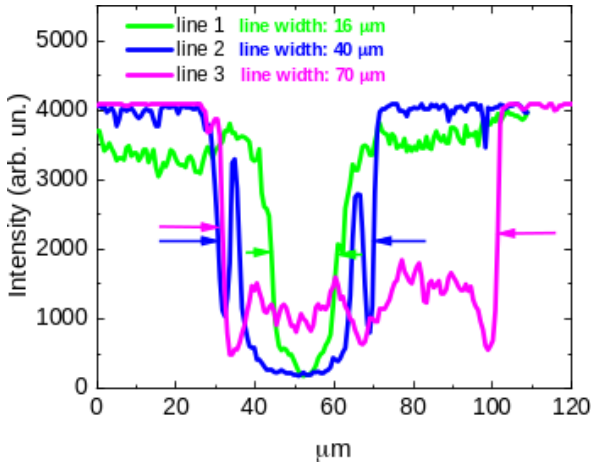

Figure 3. Intensity profiles of the images detected on the surface along the width of the lines; the measured widths are reported.

The $I(D)/I(G)$ ratio is the intensity ratio between the D and G peaks in graphene Raman spectra. The D peak represents defects or disorders in the graphene lattice, while the G peak corresponds to the graphite-like lattice vibrations. Therefore, $I(D)/I(G)$ ratio indicates the degree or disorder in the graphene structure. On the other hand, the $I(2D)/I(G)$ ratio represents the intensity ratio between the 2D peak and the G peak. The 2D peak is associated with the order in the z direction, the $I(2D)/I(G)$ ratio determines the number of graphene layers, a large value of this indicates enhanced graphene quality. Lower-quality graphene samples, such as those with a higher degree of disorder, defects, or impurities, tend to have lower $I(2D)/I(G)$ ratios. These ratios provide insights into a sample's quality, structural integrity, and number of graphene layers. From Raman spectra we obtained the $I(D)/I(G)$ and $I(2D)/I(G)$ values for the three LIG lines reported in figure 5.b. A ratio $I(2D)/I(G)$ higher than 0.5 represents the formation of graphene structure produced by LIG process.

2025 JINST 20 C09008

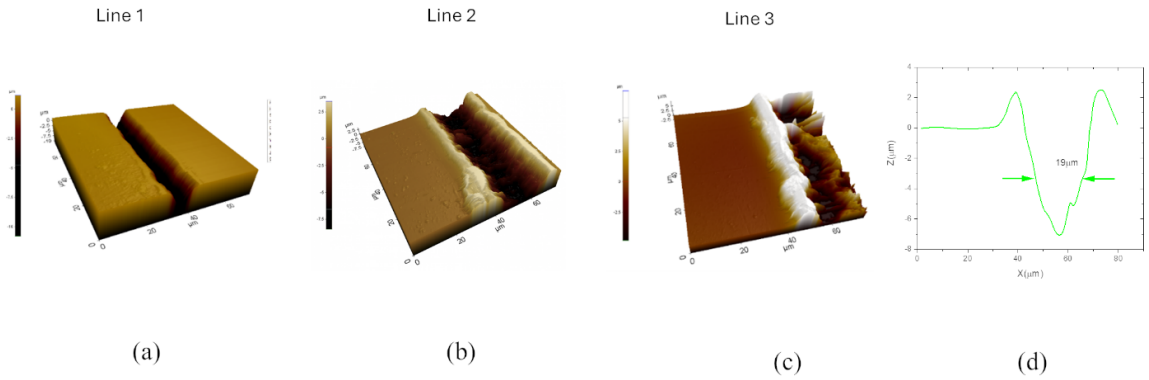

Figure 4. (a) AFM images of line 1 (a), line 2 (b) and line 3 (c). (d) Z profile of line 1.

By UV laser we obtained line with a depth under 10 µm, well below the Kapton thickness which translates into enhanced mechanical durability, that is critical for wearable sensors subjected to repeated deformation, bending, and environmental exposure during real-world use. However, by increasing laser power to obtain a complete conversion of Kapton into graphene, the line width increases diminishing the potential resolution for scribing a sensor. Therefore, to ensures graphene formation at low laser power it is necessary to vary other laser parameters as scanning speed, repetition rate etc. . .

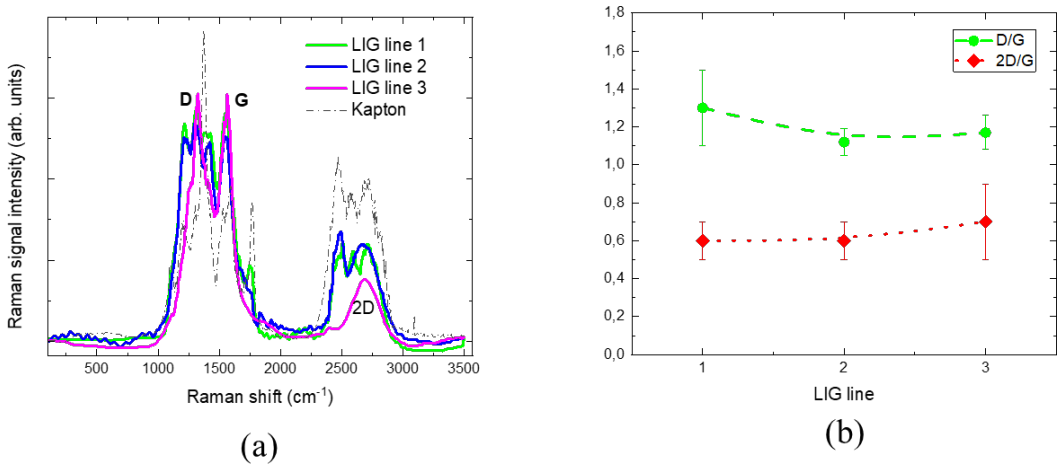

Figure 5. (a) Representative Raman spectra measured from the LIG lines. The laser power increases from line 1 to line 3. Kapton laser spectrum before irradiation is reported. (b) Raman spectra band intensity ratios $I(D)/I(G)$ and $I(2D)/I(G)$ for the three LIG lines.

4 Conclusions

We demonstrated LIG formation by direct UV laser scribing on a commercial Kapton tape. By varying laser power, different percentage of Kapton conversion into graphene were obtained. Our work demonstrates that by using Raman spectroscopy it is possible to obtain an affordable and fast feedback on the obtained graphene quality suitable for a correct tune of laser parameters.

2025 JINST 20 C09008

References

[1] Z. Zhang et al., *A review of laser-induced graphene: From experimental and theoretical fabrication processes to emerging applications*, *Carbon* **214** (2023) 118356.

[2] K. Avinash and F. Patolsky, *Laser-induced graphene structures: From synthesis and applications to future prospects*, *Mater. Today* **70** (2023) 104.

[3] A. Diaspro, *Confocal and Two-Photon Microscopy. Foundations, Applications and Advances*, A. Diaspro ed., Wiley-Liss, New York, NY, U.S.A. (2002).

[4] J. Lin et al., *Laser-induced porous graphene films from commercial polymers*, *Nature Commun.* **5** (2014) 5714.

[5] R. Ye, D.K. James and J.M. Tour, *Laser-Induced Graphene: From Discovery to Translation*, *Adv. Mater.* **31** (2018) 1704894.

[6] S. Koulouridis et al., *Ultraviolet laser-induced graphene for flexible biosensors*, *ACS Appl. Mater. Interfaces* **14** (2022) 2567.

[7] J. Liao et al., *Laser-Induced Graphene-Based Wearable Epidermal Ion-Selective Sensors for Noninvasive Multiplexed Sweat Analysis*, *Biosensors* **12** (2022) 397.

[8] Z. Wang et al., *Scalable and maskless UV laser writing of graphene for flexible electronics*, *Flex. Print. Electron.* **9** (2024) 015004.

2025 JINST 20 C09008